

Why do we need the new BNL muon $g - 2$ experiment now?

David W. Hertzog^{a*}

^aDepartment of Physics

University of Illinois at Urbana-Champaign, Urbana, IL 61801 USA

New final results from the CMD-2 and SND e^+e^- annihilation experiments, together with radiative return measurements from BaBar, lead to recent improvements in the standard model prediction for the muon anomaly. The uncertainty at 0.48 ppm—a largely data-driven result—is now slightly below the experimental uncertainty of 0.54 ppm. The difference, $a_\mu(\text{expt}) - a_\mu(\text{SM}) = (27.6 \pm 8.4) \times 10^{-10}$, represents a 3.3 standard deviation effect. At this level, it is one of the most compelling indicators of physics beyond the standard model and, at the very least, a major constraint for speculative new theories such as SUSY or extra dimensions. Others at this Workshop detailed further planned standard model theory improvements to a_μ . Here I outline how BNL E969 will achieve a factor of 2 or more reduction in the experimental uncertainty. The new experiment is based on a proven technique and track record. I argue that this work must be started now to have maximal impact on the interpretation of the new physics anticipated to be unearthed at the LHC.

1. Introduction

At the Tau-04 Workshop, I summarized [3] the recently completed Brookhaven E821 muon anomalous magnetic moment measurements and described a proposal for an extension of the measurement program. The E969 experiment [2] is designed to build on the existing infrastructure at BNL by beamline and ring improvements aimed at increasing the storable muon fraction and, simultaneously, reducing unwanted hadronic background. The goal is a reduction in the uncertainty of $a_\mu(\text{expt})$ by a factor of 2 or more. Over the past two years, the proposal plans have been scrutinized and updated. The technical plan is more complete and a prototype of one of the new detector concepts has been built and tested. During the same period, significant progress has been made in the standard model theory evaluation, as demonstrated here at Tau-06 by many authors.

The standard model expectation for the muon anomaly is based on QED, hadronic and weak loop contributions. Passera [4] reviewed the present status and introduced special topics, which were expanded on by others. Nio [5] described an ambitious effort to complete QED cal-

culations through 10th order. Vainshtein [6] focussed on the evaluation of the hadronic light-by-light (HLbL) contribution, whose present uncertainty at 0.2-0.3 ppm will become significant on the scale of the experimental goals. But the present dominant theory uncertainty is associated with the data-driven determination of the 1st-order hadronic vacuum polarization (HVP). In particular, the nagging question of why the tau hadronic decay data does not agree with the direct e^+e^- annihilation approach was raised. The problem is evident in the “single number” test to determine the $\tau^- \rightarrow \nu_\tau \pi^- \pi^0$ branching ratio. The tau result is 4.5 standard deviations higher than that predicted by CVC from e^+e^- data [7]. Isospin corrections [8] and the general QCD compatibility of tau and e^+e^- data at higher energies [9] were presented, but no resolution of the problem was offered.

The e^+e^- -based HVP situation featured new results [10] from the Novosibirsk VEPP-2M experiments CMD-2 and SND. Both independently measure the $e^+e^- \rightarrow \text{hadrons}$ cross section below the ϕ resonance. After adjusting for several subtle mistakes in the radiative correction procedures, both experiments are in excellent agreement. Complementing this direct data is the radiative return method where the e^+ and e^-

*Representing the E821 [1] and the E969 [2] Collaborations.

beams in a collider are fixed in energy and the center-of-mass collision energy is reduced by the initial-state radiation. To establish the predictive spectrum of such collisions requires a radiative correction analysis, which is made possible by the PHOKHARA Monte Carlo generator [11]. Data sets requiring this treatment come from BaBar [12] and KLOE [13]. So far, the BaBar results have mainly focussed on the high-mass region where they have improved knowledge of various exclusive many-body channels. The important $\pi\pi$ cross section near the ρ resonance is a particular challenge since the required precision to be competitive is at the sub-percent level. KLOE is focussing on just this region and it is well known that their initial report [14], which agrees in the integral with the direct annihilation measurements, is incompatible in spectral shape. Venanzone described much larger data sets that have more robust built-in cross checks (e.g., small- and large-angle sensitivity to the radiated gamma so the events can be sorted in different kinematical regions). These data are being analyzed [13] at present and we can expect results by the next Tau Workshop.

Because the HVP contributions drive the uncertainty on the standard model prediction, $a_\mu(\text{SM})$, Davier summarized [7] the situation regarding the hadronic tau decays, radiative return techniques and the new direct e^+e^- measurements. His conclusions on HVP and the other standard model contributions are compiled in Table 1. The total theoretical uncertainty is 0.48 ppm, to be compared with 0.54 ppm from the experiment. The theory uncertainty is the smaller—and, the work described here promises that it will be reduced even further in the coming years.

The comparison of experiment to theory yields

$$a_\mu(\text{expt}) - a_\mu(\text{SM}) = (27.6 \pm 8.4) \times 10^{-10},$$

a 3.3σ effect, which hints strongly of some kind of new physics contribution. Is there a more significant indicator anywhere? If we allow that massive neutrinos are now built into an updated standard model, then the answer is “no.” But, this conclusion carries a number of assumptions. It is based on a relatively new evaluation of the HVP, which

omits the first results from KLOE using the radiative return method and all the hadronic tau data [15]. The selection made is meant to choose precise, consistent data sets and it favors the direct annihilation over an indirect technique that requires corrections.

Why the hadronic tau decay approach disagrees so sharply with the direct e^+e^- method is not understood, and the subject lingers as one of the most important unsolved problems that this community should try to address. The tau-based HVP data determine an a_μ that is much closer to experiment, so it is clearly important to understand. We are lead to dismissing it for now by the tau proponents [15] who argue that uncertainties in the treatment of isospin corrections, perhaps manifest by the spectral shape inconsistency between tau and e^+e^- data, are uncertain at the required level of accuracy. Further, the CVC test fails miserably. Something is not right and the confusion clouds the stated theoretical a_μ as quoted. If the standard model is accurately represented by the e^+e^- data, then the $(g-2)$ test is very suggestive of new physics. Based on this interpretation—it is not a guarantee, only a very good bet—the Collaboration feels strongly that a compelling motivation to improve the a_μ measurement exists. Of course it is imperative to resolve the tau issue and to corroborate the direct e^+e^- data with at least one of the radiative return methods from KLOE, BaBar or Belle; but, this work continues and we can expect results in the near term.

2. E821 Summary

The E821 data taking was completed in 2001 and the final analyses are all published [20,21,22,23,24]. A comprehensive summary of the experiment, containing many of the details of the methods used for data taking and analysis, was published [19] and a more general review is also available [25]. With nearly equally precise a_μ determinations from positive and negative muon samples, the CPT-combined final result is $a_\mu^\pm = 11\,659\,208(6) \times 10^{-10}$. The statistical and systematic uncertainties are combined in quadrature.

A precision measurement depends on control

Table 1
2006 Standard model theory and experiment summarized at this Workshop [7]

Contribution	Value $\times 10^{10}$	Error $\times 10^{10}$	Reference	Comment
QED	11 658 471.9	0.1	[16,5]	4 loops; 5th estimated; see Nio
Hadronic vacuum polarization	690.9	4.4	[7]	Only CMD-2 and SND used
Hadronic light by light	12.0	3.5	[18]	Value from Ref. [17]
Hadronic, other 2nd order	-9.8	0.1	[15]	
Weak	15.4	0.22	[17]	2 loops
Total theory	11 659 180.4	5.6	[7]	0.48 ppm
Experiment	11 659 208.0	6.3	[19]	0.54 ppm
Expt. - Thy.	27.6	8.4	-	3.3 standard deviations

of the systematic uncertainties. These errors were reduced in magnitude in each of the running years. We group the uncertainties into those related to ω_a , the precession frequency extraction, and those related to ω_p , the determination of the average magnetic field. The achieved uncertainties were 0.21 ppm and 0.17 ppm, respectively (with numerous sub-categories contributing to each class of error). The goal for the new experiment is to limit the precession and field systematic uncertainties each to 0.1 ppm. This will require new data taking operation modes of the storage ring to reduce some of the more important beam-dynamics related uncertainties and the installation of higher-granularity detectors to reduce the pile-up (instantaneous) rate correction. The field uncertainty improvements will be achieved by a continued refinement of the present operation of shimming, measuring, and monitoring.

3. How is $g-2$ measured?

The modern method to determine the muon anomalous moment is to measure the difference frequency ω_a between the spin precession and the cyclotron motion of an ensemble of polarized muons, which circulate a storage ring in a highly uniform magnetic field. Apart from very small corrections, ω_a is proportional to a_μ . Vertical containment is achieved by electric quadrupoles. Therefore, the muon spin can be affected by the motional magnetic field. Formally, in the presence of a magnetic and electric field having

$\vec{B} \cdot \vec{\beta} = \vec{E} \cdot \vec{\beta} = 0$, ω_a is described by

$$\begin{aligned} \vec{\omega}_a &\equiv \vec{\omega}_s - \vec{\omega}_c \\ &= \frac{e}{m_\mu c} \left[a_\mu \vec{B} - \left(a_\mu - \frac{1}{\gamma^2 - 1} \right) (\vec{\beta} \times \vec{E}) \right] \end{aligned} \quad (1)$$

where $\vec{\beta}$ represents the muon direction and ω_s and ω_c are the spin and cyclotron frequencies, respectively. The term in parentheses multiplying $\vec{\beta} \times \vec{E}$ vanishes at $\gamma = 29.3$ and the electrostatic focussing does not affect the spin (except for a correction necessary to account for the finite momentum range $\Delta P/P \approx \pm 0.14\%$ around the magic momentum). Equation 1 can be rearranged to isolate a_μ , giving ω_a/B multiplied by physical quantities that are known to high precision.

The magic momentum sets the scale of the experiment and the BNL storage ring [26] is 7.1 m in radius and has a 1.45 T magnetic field. At 3.094 GeV/c the time-dilated muon lifetime is 64.4 μs , and the decay electrons² have an upper lab-frame energy of approximately 3.1 GeV. A key feature of the experiment is the injection of a short pulse of polarized muons, which enter the ring tangent to, but offset from, the central storage radius. They are kicked transversely to align with a trajectory concentric with the ring center.

The rate of detected electrons having an energy greater than a set threshold is an exponential (as above), but modulated at the anomalous

²By convention, we discuss negative muons and their decay electrons throughout this paper.

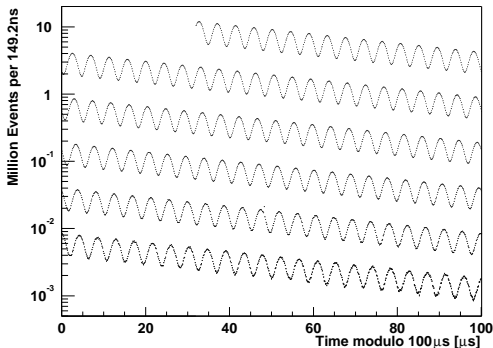


Figure 1. Distribution of counts versus time for the 3.6 billion decays in the 2001 negative muon data-taking period.

precession frequency, ω_a , see Fig. 1. The key to the experiment is to determine this frequency to high precision and to measure the average magnetic field to equal or better precision. The field is determined from a suite of NMR measurements [27,28] using calibration, fixed and movable probes to reference the field against a known standard, to monitor the field continuously, and to map the field in the storage ring aperture, respectively. The techniques are documented in Ref. [19].

4. Steps toward an improved g-2 measurement

The key to improving on the E821 experiment is obtaining more stored muons, lowering the hadronic-induced background, and managing the high instantaneous rate at the time of the fit start, approximately $25 \mu\text{s}$ after injection. The plan assumes running at the average proton intensity of 50 Tp/cycle achieved in E821. Although it introduces no new extraordinary demands on the AGS complex, five years have passed since high-intensity proton running has occurred and this mode of operation will have to be re-established. Outlined below is a relatively conservative set of upgrades for the new experiment, the core of

which forms the theme in the proposal [2]. The more creative “backward” decay beam concept (see also Ref. [3]) is not described here because technical and cost uncertainties must be better understood before we commit to its implementation. Instead, a simple and largely tested “forward” decay scheme, along with several new ideas that have recognized advantages, are presented.

4.1. Greater bunch rate

The ideal experiment divides the accelerator proton budget into a large number of short-bunch-length pulses per cycle. Each bunch generates an independent muon “fill.” Twelve bunches per 2.7 s cycle is the normal operation at the AGS. With a muon fill lasting no more than 1 ms, the experiment is “on” only 0.44 percent of the time. The instantaneous rate exceeds several MHz per detector and already implies a significant pileup correction of a few percent. As the stored muon rate must increase to achieve the statistical goal, the pileup fraction must not increase, which can be realized by subdividing the detectors and/or decreasing the average rate per bunch. The latter implies a higher bunch rate per cycle, which places new demands on the AGS operations. A scheme worked out many years ago splits the primary 12 bunches spatially into three distinct co-moving components. Each “sub-bunch” is extracted independently. This operation is not yet a tested concept, and it likely requires new extraction hardware. But, it is an attractive idea that would improve the experiment tremendously if it can be realized.

4.2. Improved muon collection

The pion-muon beamline upstream of the ring has three components: a pion creation and collection section; a pion-to-muon decay section; and a final muon selection at $P_{magic} = 3.094 \text{ GeV}/c$. Figure 2 is a schematic of the beamline and storage ring. A number of competing factors enter into final figure-of-merit (loosely defined as muons into the ring times average polarization squared times fraction stored). The numbers given below have all these factors folded together into a simple “stored muon” factor.

The pion collection and muon selection sections

are tuned to slightly different momenta. Typical operating conditions in E821 set the pion momentum 1.7% greater than P_{magic} . Forward decay muons, but slightly off axis from zero degrees, are contained in the decay channel and transported through the final bending arc indicated by dipoles D5 and D6, which are tuned to the P_{magic} momentum. These muons have a longitudinal polarization of $\approx 94.5\%$. The slightly higher momentum pions that enter the final arc are largely cut at the K3/K4 slit; however, the low-momentum tail of the pion distribution is transported through the slits and into the ring. The pion-to-muon ratio is typically 1:1 at nominal settings, but this ratio can be controlled by many factors. At the first pion collection arc, slits K1/K2 define a pion momentum acceptance. In operation, a narrow $\Delta P/P$ of $\approx 0.5\%$ was used. Higher flux can be obtained, but only at the expense of higher pion contamination at the final K3/K4 selection as well. In contrast, increasing the P_π/P_{magic} ratio reduces both the muon and pion flux entering the ring, with the pion contamination falling typically faster and therefore improving the muon purity.

Under the best operating conditions, the pion flux still created a prompt “hadronic flash” in E821, which was followed by a slower neutron capture time lasting 10’s of microseconds. This background particularly affected the calorimeters placed near the injection side of the ring and had the effect of limiting the start time of the physics fits. The plan described for E969 will decrease the absolute number of pions entering the ring per fill by increasing the P_π/P_{magic} ratio.

Since the submission of the proposal, we have worked extensively on improving the beam transport modeling studies, especially in the 80-m long pion-to-muon FODO decay section. An optimization has been developed with respect to the hardware changes (more quadrupoles) and the tuning of momenta and slit acceptances. Our current conclusions [29] suggest that quadrupling the number of quadrupole elements will help collect more useful muons. Figure 3 shows a 2nd-order TRANSPORT study indicating the envelope of the transported pions from the 1st arc through the FODO section. The spatial extent

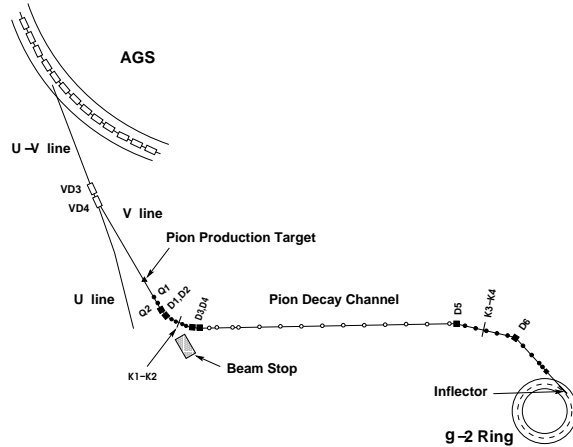


Figure 2. Plan view of the pion/muon beamline.

is much smaller compared to the current line, allowing the collection of a larger fraction of muons to fill the beamline phase space (essentially, a larger divergence will be accepted because the spatial deviation of the decay coordinate is always kept small). Starting with the assumption that the ratio P_π/P_{magic} is raised to 1.03, the effective improvement in muon flux times polarization squared is approximately 3.3. If estimates of the final ring acceptance are included, it is reduced to ≈ 2.5 . But, the pion flux will have dropped by roughly a factor of 3 for this choice of momentum ratio. In practice, the final numbers will be tuned to optimize conditions. The studies leading to these conclusions were drawn from modeling using DECAY TURTLE and TRANSPORT, both standard beam-design tools [30].

4.3. Improved muon transmission through the inflector

The muon beam enters the storage ring through a superconducting inflector [31]. The inflector has coils that essentially block both the entrance and exit openings. Studies show that energy loss and multiple scattering prevents approximately half of the muons from being stored. Opening

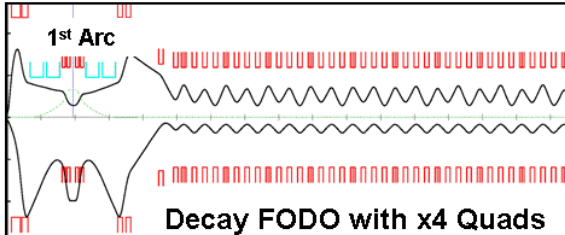


Figure 3. Beamline model of first arc and FODO section with four times the present number of quadrupoles. The envelopes represent the outer contained extent of the transported pions. The top (bottom) panel represents the horizontal (vertical) plane. The pions are constrained to lie near the optical axis, which leads to a higher fraction of collected decay muons. To fill the phase space of the channel, the accepted muon divergence can be larger for a smaller initial spatial displacement.

the ends of the inflector will recover these muons. The closed-ended inflector will be replaced by an open-ended version, which had already been prototyped and tested prior to the start of E821. The production of a full-scale open-ended inflector was reviewed during the last two years and appears to be quite feasible to build.

4.4. Improved muon storage efficiency

The muon storage efficiency is largely governed by the kicking and scraping operations. In the latter, the quadrupoles [32] are asymmetrically charged to displace the stored beam so that its outside edges strike round collimators, which define the storage volume (or aperture). The scraping process is engaged at the beginning of a fill and it is turned off in 5-10 μs . The more severe the scraping, the fewer the remaining fraction of muons; conversely, these muons are well contained, minimizing time-dependent losses during the fill. In practice, the scraping removes roughly 10 percent of the initially stored muons. While novel ideas have been projected for new scraping schemes, we simply scale the new exper-

iment with no implied improvement here in rate or background reduction.

An “ideal” kicker would provide a perfectly timed ≈ 10 mrad transverse deflection to the incoming muon bunch one quarter of a betatron wavelength after the injection. The kicker perturbation would then vanish in 149 ns, before the muons circulate the ring once. Improvement in the stored efficiency can be realized if the actual kicker system [33] can better mimic this ideal. The E821 device was made of three independent pairs of parallel current sheets (aluminum plates). Each set is rapidly energized by an LCR pulse-forming network to induce a high current and consequent vertical magnetic field. The kicker shape is shown in Fig. 4. Superimposed is a schematic representation of the time and width of the muon bunch as it passes the location of a single kicker section. The kicker shape and magnitude—already a non-trivial engineering effort to achieve—is evidently too wide. It is also not strong enough. Consequently, a smaller fraction of muons is stored and these muons are not perfectly centered by the kick—a fact that becomes evident in the data where coherent betatron oscillations appear as an underlying modulation to the nominal terms required to fit the spectra shown in Fig. 1. Simulations using an ideal kicker pulse promise a storage efficiency of approximately 8 percent (or more). The E821 kickers store $\approx 2-4$ percent, so there is clear room for improvement. This will require revisions of the electrical charging circuits, especially in the area of reduced inductance (to narrow the pulse) and some method to increase the maximum plate voltage. Clearly, any improvement in the kicker has a direct effect on the rate and quality of the stored muons. An aggressive R&D program could likely lead to a factor of 2 in increased stored muons. The focus would be on the reduction in the inductance at the pulse-forming network stage (a clear possibility exists) and by increasing the number of individual kicker sections (either shorter sections, or one additional full-sized section).

4.5. Improvements to data taking

A higher muon rate, and a substantially larger data set, require rethinking the data-taking strat-

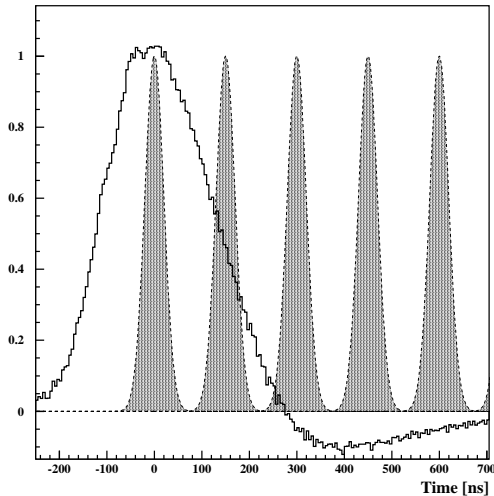


Figure 4. A kicker pulse. The periodic pulses represent the unmodified muon bunch intensity during the first few turns.

egy. In E821, 24 lead-scintillating fiber electromagnetic calorimeters [34] were used to detect electron energy and time of arrival, each read out by a single waveform digitizer (WFD). The offline programs found pulses and corrected for pileup (see Ref. [19]). A systematic uncertainty from incomplete pileup subtraction will be exacerbated at the rates expected for E969; therefore, a new segmented calorimeter that can isolate simultaneous events and a parallel method of analysis that is intrinsically immune to pileup, have been developed. Both will require more modern and higher-rate sampling waveform digitizers with deep memories.

A prototype of the new calorimeter was built and tested. It is made of alternating layers of 0.5 mm scintillating fiber ribbons and flat tungsten plates. The high density yields a Molière radius of ≈ 1.7 cm and a radiation length of ≈ 0.7 cm. The compact design is necessary so that the calorimeter front face can be divided into 20 individual detectors and read out on the

downstream side. GEANT studies show that pileup events can be recognized 4 out of 5 times, which exceeds our requirement. Results of a brief beam test, using electrons from 125 to 300 MeV at PSI, show a resolution of approximately $14\%/\sqrt{E}$, in line with simulations. The detailed balance between improved resolution (increase the scintillator to tungsten ratio, and/or reduce the layer thicknesses) and retaining the compact nature of the detector, continues to be studied. A plot of a 300 MeV electron striking the detector end-on (i.e. 5-degrees with respect to the fiber axis, as would be typical in this geometry), is shown in Fig. 5.

New waveform digitizers were designed for our PSI “MuLan” experiment [35], which aims to measure the positive muon lifetime to 1 ppm precision. A system of 340, 500-MHz waveform digitizers [36] is presently fully operational and tested. These digitizers can be programmed to meet application specific goals and we expect to use them as a standard for reading out the 480 photomultiplier tubes implicit in the E969 plan. In addition, stable clocks and a complete clock distribution network are already in hand as is a fully appropriate, high-rate data acquisition system.

A new method of acquiring data will be carried out in parallel to our traditional method. It relies on a simple integration of the energy flow versus time in each fill. No separate events are recorded, only the energy absorbed by a calorimeter versus time. The average electron energy striking a calorimeter is modulated at the ω_a frequency because of the association of electron energy with muon spin direction. The asymmetry is approximately half that of the traditional “event” method and all events striking the calorimeter contribute. Detailed GEANT simulations indicate that this data set will be statistically weaker by about 9 percent compared to the traditional method. However, it requires no pileup correction and it is statistically partially independent. The new method will provide additional information and a strong cross-check on the main analysis.

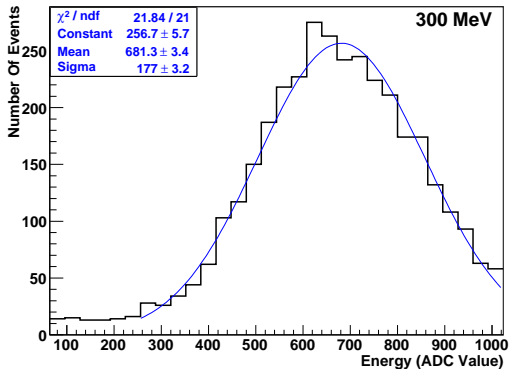


Figure 5. First tests with of a prototype W/SciFi ribbon calorimeter using a 300 MeV electron beam at PSI. The solid line is a Gaussian fit to the data. Its width corresponds to a resolution of $\approx 14\%/\sqrt{(E)}$, which was predicted from our GEANT simulations.

4.6. Summary of improvements

The new E969 experiment will require an integrated stored muon flux roughly 10 times that of E821. We assume a factor of 5 is required in the stored muon rate per AGS cycle, coupled with a running period of approximately 20 weeks. The improvements outlined increase the stored muon rate and reduce the hadronic-induced background. The instantaneous rate increase must be compensated by a combination of multi-bunch extraction and detector subdivision. The summary of improvements described in terms of expected factors is given in Table 2. Notice a stored muon rate increase of 10 is achieved, which exceeds our design goal with a safety margin of a factor of 2.

5. Summary

Why do we need the new BNL muon $g-2$ experiment now? The reasons are clear:

- The experiment can be improved by at least a factor of 2 but it must be started “now” to be ready when the results from the LHC will demand additional constraints. Several years of R&D and construction are required before running and analysis can begin. We estimate roughly 5 – 6 years from project start to achieve the goal.
- The standard model theory uncertainty is already slightly smaller than experiment and it should be halved again over the next few years. The improvements have been driven by the fact that real measurements of a_μ were also being made. The momentum should be sustained and new efforts, especially related to the difficult hadronic light-by-light contribution, must be encouraged. It is quite likely that the next sophisticated step will employ lattice QCD techniques.
- We are already at a compelling moment. The present (e^+e^- -based theory) is 3.3 standard deviations from the experiment, providing a strong hint of new physics. If the current discrepancy of 27.6×10^{-10} persists, with halved experimental and theoretical uncertainties, the significance will rise to 6.7σ .
- For specific models, such as SUSY, a_μ is particularly effective at constraining $\tan \beta$ —the ratio of Higgs vacuum expectation values—for a given superparticle mass. This information will be complementary to the anticipated LHC new-particle spectra and it will be crucial in the effort to pin down the parameters of the theory behind them.
- Independently of SUSY—we do not suggest or depend on this or any other specific model as being correct—measuring a_μ to very high precision will register an important constraint for any new physics theory to respect. Some models will predict a large ($g-2$) effect, while others will not. It is information that can likely help diagnose new physics.
- On the practical side, the project is based on a proven track record by an existing team of experts and new enthusiastic collaborators. It is efficient to mobilize

Table 2

Summary of improvements compared to E821, where N , B and R represent the overall stored muon figure of merit, the relative hadron-induced background, and the initial instantaneous rate, respectively.

Improvement	N	B	R	Comment
AGS bunch increase	1	1	0.33	An attractive possibility, but uncertain
Quadruple FODO quads	2.5	0.33	2.5	Detailed studies at $P_\pi/P_{magic} = 1.03$
Open inflector end	2	1	2	Preliminary studies support conclusion
Kicker	2	1	2	Simulations in progress; engineering required
Summary	10	0.33	3.3	

the Collaboration now while the ring and beamline facilities can be dependably recommissioned, and while the diverse expertise exists.

6. Acknowledgments

The $(g - 2)$ experiment is supported in part by the U.S. Department of Energy, the U.S. National Science Foundation, the German Bundesminister für Bildung und Forschung, the Russian Ministry of Science, and the US-Japan Agreement in High Energy Physics.

REFERENCES

- Muon E821 Collaboration: G.W. Bennett, B. Bousquet, H.N. Brown, G. Bunce, R.M. Carey, P. Cushman, G.T. Danby, P.T. Debevec, M. Deile, H. Deng, W. Deninger, S.K. Dhawan, V.P. Druzhinin, L. Duong, E. Efstathiadis, F.J.M. Farley, G.V. Fedotovitch, S. Giron, F.E. Gray, D. Grigoriev, M. Grosse-Perdekamp, A. Grossmann, M.F. Hare, D.W. Hertzog, X. Huang, V.W. Hughes M. Iwasaki, K. Jungmann, D. Kawall, M. Kawamura, B.I. Khazin, J. Kindem, F. Krienen, I. Kronkvist, A. Lam, R. Larsen, Y.Y. Lee, I. Logashenko, R. McNabb, W. Meng, J. Mi, J.P. Miller, Y. Mizumachi, W.M. Morse, D. Nikas, C.J.G. Onderwater, Y. Orlov, C.S. Özben, J.M. Palley, Q. Peng, C.C. Polly, J. Pretz, R. Prigl, G. zu Putlitz, T. Qian, S.I. Redin, O. Rind, B.L. Roberts, N. Ryskulov, S. Sedykh, Y.K. Semertzidis, P. Shagin, Yu.M. Shatunov, E.P. Sichtermann, E. Solodov, M. Sossong, A. Steinmetz L.R. Sulak, C. Timmermans, A. Trofimov, D. Urner, P. von Walter, D. Warburton, D. Winn, A. Yamamoto and D. Zimmerman; See Refs. [19,20,21,22,23,24].
- A $(g - 2)_\mu$ Experiment to ± 0.2 ppm Precision, R.M. Carey, A. Gafarov, I. Logashenko, K.R. Lynch, J.P. Miller, B.L. Roberts (co-spokesperson), G. Bunce, W. Meng, W.M. Morse (resident spokesperson), Y.K. Semertzidis, D. Grigoriev, B.I. Khazin, S.I. Redin, Yuri M. Shatunov, E. Solodov, Y. Orlov, P. Debevec, D.W. Hertzog (co-spokesperson), P. Kammel, R. McNabb, F. Müllhauser, K.L. Giovanetti, K.P. Jungmann, C.J.G. Onderwater, S. Dhamija, T.P. Goringe, W. Korsch, F.E. Gray, B. Lauss, E.P. Sichtermann, P. Cushman, T. Qian, P. Shagin, S. Dhawan and F.J.M. Farley.
- David W. Hertzog, Nucl. Phys. B (Proc. Suppl.) **144**, 191 (2005).
- M. Passera, This Workshop.
- M. Nio, This Workshop.
- A. Vainshtein, This Workshop.
- M. Davier, This Workshop.
- G. Lopez Castro, This Workshop.
- K. Maltman, This Workshop.
- S. Eidelman, This Workshop.
- G. Rodrigo, This Workshop, also see: <http://grodrigo.web.cern.ch/grodrigo/phokhara/>.
- W. Wang, This Workshop.
- G. Venanzoni, This Workshop.
- A. Aloisio, et al., (KLOE Collaboration) Phys. Lett. **B606**, 12 (2005).
- M. Davier, S. Eidelman, A. Höcker, and Z. Zhang, Eur. Phys. J. **C 31**, 503 (2003).
- T. Kinoshita and M. Nio, Phys. Rev. Lett. **90**, 021803 (2003) and T. Kinoshita and M. Nio, Phys. Rev. **D70**, 113001 (2004).
- M. Davier and W. Marciano, Annu. Rev.

- Nucl. Part. Sci. **54** 115 (2004).
18. J. Bijnens, E. Pallante and J. Prades, Nucl. Phys. **B474**, 379 (1996) and Nucl. Phys. **B626**, 410 (2002); M. Hayakawa and T. Kinoshita, Phys. Rev. **D57**, 465(1998) and hep-ph/0112102 (2002); M. Knecht, A. Nyffeler, Phys. Rev. **D65**, 073034 (2002); M. Knecht, A. Nyffeler, M. Perrottet, E. De Rafael, Phys. Rev. Lett. **88**, 071802 (2002); I. Blokland, A. Czarnecki and K. Melnikov, Phys. Rev. Lett. **88**, 071803 (2002); K. Melnikov and A. Vainshtein, Phys. Rev. **D70**, 113006 (2004). We use the recommended value in Ref. [17].
 19. The $g-2$ Collaboration: G.W. Bennett et al., Phys. Rev. D **73** (2006) 72003.
 20. The $g-2$ Collaboration: R.M. Carey et al., Phys. Rev. Lett. **82**, 1132 (1999).
 21. The $g-2$ Collaboration: H.N. Brown et al., Phys. Rev. **D62**, 091101 (2000).
 22. The $g-2$ Collaboration: H.N. Brown et al., Phys. Rev. Lett. **86**, 2227 (2001).
 23. The $g-2$ Collaboration: G.W. Bennett et al., Phys. Rev. Lett. **89** (2002) 101804; Erratum-ibid. **89** (2002) 129903.
 24. The $g-2$ Collaboration: G.W. Bennett et al., Phys. Rev. Lett. **92** (2004) 161802.
 25. D.W. Hertzog and W.M. Morse, Annu. Rev. Nucl. Part. Sci. **54** 141 (2004).
 26. G.T. Danby, et al., Nucl. Instr. and Methods Phys. Res. **A 457**, 151-174 (2001).
 27. R. Prigl, et al., Nucl. Inst. Methods Phys. Res. **A374** 118 (1996); X. Fei, V. Hughes and R. Prigl, Nucl. Inst. Methods Phys. Res. **A394**, 349 (1997).
 28. W. Liu et al., Phys. Rev. Lett. **82**, 711 (1999).
 29. ($g-2$) Internal Study, March 2006, P. Kammer and P. Pile.
 30. U. Rohrer (PSI) versions based on K.L. Brown, Ch. Iselin, D.C. Carey, *Decay Turtle*, CERN 74-2 (1974); and K.L. Brown, D.C. Carey, Ch. Iselin and F. Rothacker *Transport, a Computer Program for Designing Charged Particle Beam Transport Systems*, CERN 73-16 (1973) and CERN 80-04 (1980).
 31. F. Krienen, D. Loomba and W. Meng, Nucl. Inst. and Meth. **A 283**, 5 (1989); A. Yamamoto, et al., Nucl. Instrum. and Methods Phys. Res. **A491** 23-40 (2002).
 32. Y.K. Semertzidis, Nucl. Instrum. Methods Phys. Res. **A503** 458-484 (2003).
 33. E. Efstathiadis, et al., Nucl. Inst. and Methods Phys. Res. **A496** ,8-25 (2002).
 34. S.A. Sedykh et al., Nucl. Inst. Methods Phys. Res. **A455** 346 (2000).
 35. PSI Experiment R99.07.01 *A Precision Measurement of the Positive Muon Lifetime Using a Pulsed Muon Beam and the μ Lan Detector* R.M. Carey, et al.; R. Carey and D. Hertzog, (co-spokespersons).
 36. 500 MHz waveform digitizers, built by R. Carey, K. Lynch, and W. Earle at Boston University.